

EMPIRICAL MODELS FOR LOSSES CALCULATION IN A RECTANGULAR DUCT EQUIPPED BY ARTIFICIAL ROUGHNESS

N.CHOUCHANE*, A.MOUMMI*, A.BRIMA**, N.MOUMMI**

*Civil Engineering, Hydraulics Laboratory, Development Sustainability and Environment (LAR-GHYDE), University of Mohamed Khider-Biskra
 **Mechanical Engineering Laboratory(LGM), University of Mohamed Khider-Biskra
 ch_nacer@yahoo.fr

ABSTRACT

The objective of this work is to find empirical models linking load losses to the geometric characteristics of artificial roughness called baffles and different modes of provisions of these fluids in the vein of a rectangular channel.

An experimental design was set up to measure the losses Load caused by baffles between the upstream and downstream of the channel. The experimental measurements made have enabled us to establish empirical relationships to evaluate losses in accordance with load losses configuration and arrangement of baffles and for different flow regimes.

KEYWORDS: losses, correlation, artificial roughness, solar collector, convective exchanges.

1 INTRODUCTION

In order to optimize the convective heat transfer in heat exchangers and solar air flat plate collector, we introduce obstacles with a variety of shapes into the duct, which contribute to heat transfer by conduction, convection and radiation.

However, their presence is induced by a considerable increase in load losses, which depends on the shape and geometry disposition into the conduit.

To study the effect of fins on the load losses, many research frame work have been begun.

Bhagoria et al. (2002) [1], Karwa et al. (1998) [2] have studied the influence of artificial roughness on the load losses and their effect on thermal performance when the air flow is in a rectangular channel.

They tested transverse obstacles with an upper portion inclined, where they examined the variation of load losses according to the spacing distance between rows, the relative roughness and the angle of inclination.

Chaube et al. (2006) [3] and Apura et al. (2009) [4] studied continuous transverse obstacles with a portion inclined and not inclined, a comparative study has been initiated between the configurations considered and the smooth case.

Cavallero et al. (2002) [5], Giovanni Tanda (2004) [6] considered obstacles staple, they examined the variation of load losses according to the layout geometry, such that the spacing between the obstacles and the rows, the relative roughness and the length of the obstacles, the results of different configurations obtained were compared with the smooth, case

Nomenclature

ΔP	Load losses [Pascal]
V	Fluid velocity in the duct [m / s]
ε	Absolute roughness [m]
P_{e-ch}	Step between ribs (obstacles) [m]
C.R	Rectangular rib (obstacle)
C.R.T	Rectangular- triangle rib(obstacle) .
$P_{e-s.ch}$	Step between the tops of ribs (obstacles) [m]
P_{e-r}	Not between two successive rows of ribs (obstacles) [m]
C.R.Tr	Rectangular trapezoidal rib (obstacle)
ρ	Fluid density [kg/m ³]
μ	Dynamic viscosity [Kg / m.s]
L	Channel length [m]
L_{ch}	Length of a rib (obstacle) [m]
C .T	Triangular rib (obstacle)

Jaurker et al .(2006)[7], used thick blades that have grooves made between two ribs, in their investigation examined the influence of the variation in the spacind distance between a rib and a groove, also the effect caused by roughness on the load losses.

In this experimental study, four configurations of obstacles Fig. (02) have been tested, are provided with an upper portion inclined Fig. (4 a) to create disordered flow with vortex structure in vertical and horizontal axis, due to a multitude of sharp contraction and expansion, particularly with the staggered arrangement figure (4 b) .

2 EXPERIMENTAL DEVICE

The experimental device is designed in the Department of Mechanical Engineering in University of Biskra. It is a rectangular duct of 2.5 m long, 0.5 m wide and a height of 0,025 m in which ribs are introduced in length respectively 5, 7 and 10 cm, arranged in the useful space of flow of fluid (water). The ribs are cut galvanized steel 0.4 mm thick, arranged in rows and staggered rows see fig. (4). The related spaces between two successive rows are considered equal to 25, 18, 14, 10, and 05 cm. On the other hand, the related spaces not on the between the summits of two successive baffles in the same row are 15, 10 and 08 cm. The spaces between two ribs in the same row are 10, 07, 05 and 03 cm.

The ribs include two integral parts. One part fixed orthogonally to the plane flow of 01 cm in length, cons by the inclined portion is 1.5 cm see fig. (2), the implications of the upper part is 30 °, 60 °, 120 ° and 150

Measurements of losses have been taken at first for a smooth channel (without ribs) for different flow values. In the second step, the same measurements were taken for the considered configurations of ribs see fig. (2), arranged in rows then staggered rows

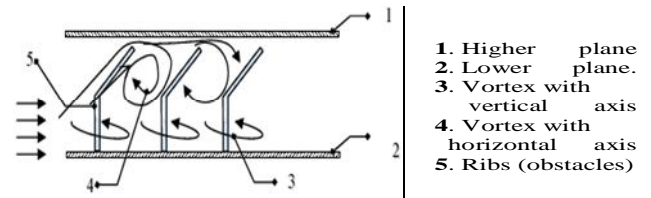


Figure 3: Scheme of the impact of fluid in the vicinity of the ribs

3 EMPIRICAL MODEL FOR CALCULATING LOAD LOSSES

The results obtained show that the losses recorded are becoming more and more prominent with the number of rows of ribs, especially the effects of 60 and 120 ° of the upper slope, when pitch on the ribs and between the rows is reduced. They are particularly more important in the presence of the provision in staggered rows see fig. (4) (b) when they are aligned in rows see fig. (4) (a).

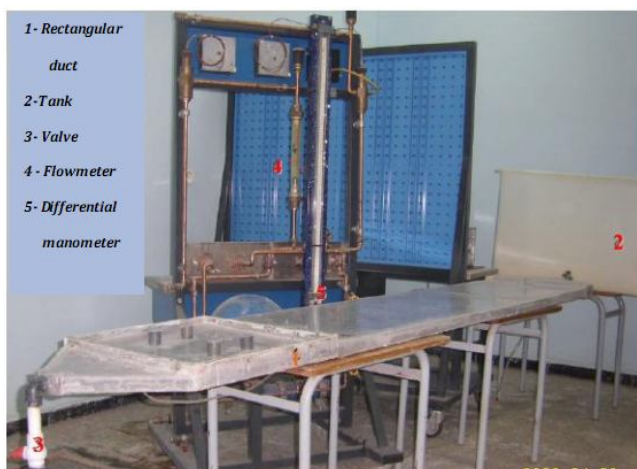


Figure 1: Experimental measurement of load losses

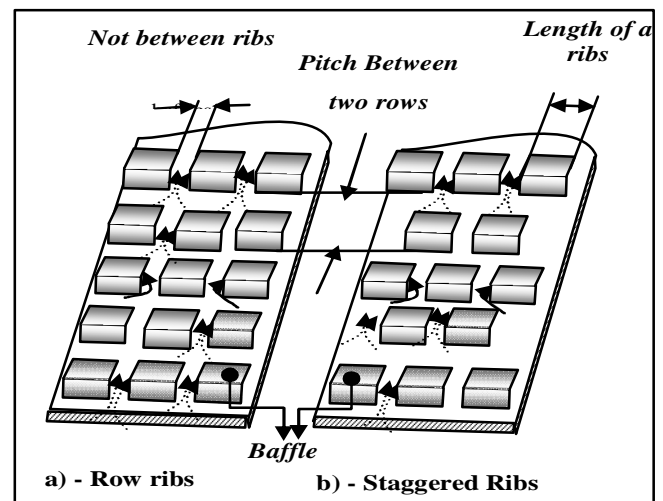


Figure 4: Arrangement of ribs in rows and staggered rows

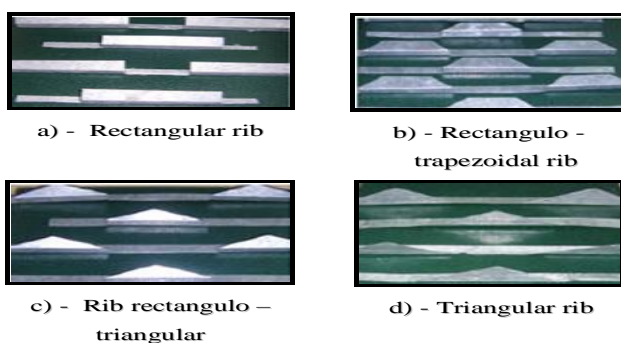


Figure 2: configuration of studied baffles

To correlate the losses to the geometric characteristics of the ribs, to the physical parameters of fluid flow, and geometry of provisions in the lead useful, we have used the method of dimensional analysis (Vashy Buckingham's theorem) [1], which provides a general relationship based on the fundamental dimensions of the form:

$$\Delta P = \Delta P \left(\rho, D_H, V, \mu, \varepsilon, L, P_{e-ch}, P_{e-r}, L_{ch}, P_{e-sch} \right) \quad (1)$$

According to the theorem π (Vashy-Bukingham), we can only have seven (07) independent groups, so we adopt the following representation, and knowing that the length of the rectangular duct L is constant.

$$\frac{\Delta P}{L} = \left(\begin{array}{c} \pi . k . \rho^\alpha . D_H^\beta . V^\gamma . \mu^x . \varepsilon^y \\ . P_{e-ch}^z . P_{e-r}^t . L_{ch}^\omega . P_{e-sch}^n . ch \end{array} \right) \quad (2)$$

The writing of equation (2), given the basic dimensions, and after the development and identification has enabled us to get a system of 03 equations, whose resolution leads to a general expression of the form:

$$\Delta P = \frac{1}{2} \frac{L}{D_H} \rho V^2 \left[\begin{array}{c} \left(\frac{\rho V . D_H}{\mu} \right)^{-x} \left(\frac{\varepsilon}{D_H} \right)^y \left(\frac{P_{e-ch}}{D_H} \right)^z \\ \times \left(\frac{P_{e-r}}{D_H} \right)^t \left(\frac{L_{ch}}{D_H} \right)^\omega \left(\frac{P_{e-sch}}{D_H} \right)^n \end{array} \right] \quad (3)$$

When we introduce Reynolds' number, expression (3) becomes:

$$\Delta P = \frac{1}{2} \frac{L}{D_H} \rho V^2 \left[\begin{array}{c} (Re)^{-x} . \left(\frac{\varepsilon}{D_H} \right)^y . \left(\frac{P_{e-ch}}{D_H} \right)^z \\ \times \left(\frac{P_{e-r}}{D_H} \right)^t . \left(\frac{L_{ch}}{D_H} \right)^\omega . \left(\frac{P_{e-sch}}{D_H} \right)^n \end{array} \right] \quad (3')$$

The term in brackets represents the ratio of losses λ expressed as:

$$\lambda = \left[\begin{array}{c} (Re)^{-x} \left(\frac{\varepsilon}{D_H} \right)^y \left(\frac{P_{e-ch}}{D_H} \right)^z \\ \times \left(\frac{P_{e-r}}{D_H} \right)^t \left(\frac{L_{ch}}{D_H} \right)^\omega \left(\frac{P_{e-sch}}{D_H} \right)^n \end{array} \right] \quad (4)$$

$$\ln \frac{2 \Delta P D_H}{L \rho V^2} = \left[\begin{array}{c} -x \ln(Re) + y \ln \frac{\varepsilon}{D_H} \\ +z \ln \frac{P_{e-ch}}{D_H} + t \ln \frac{P_{e-r}}{D_H} \\ +w \ln \frac{L_{ch}}{D_H} + n \ln \frac{P_{e-sch}}{D_H} \end{array} \right] \quad (5)$$

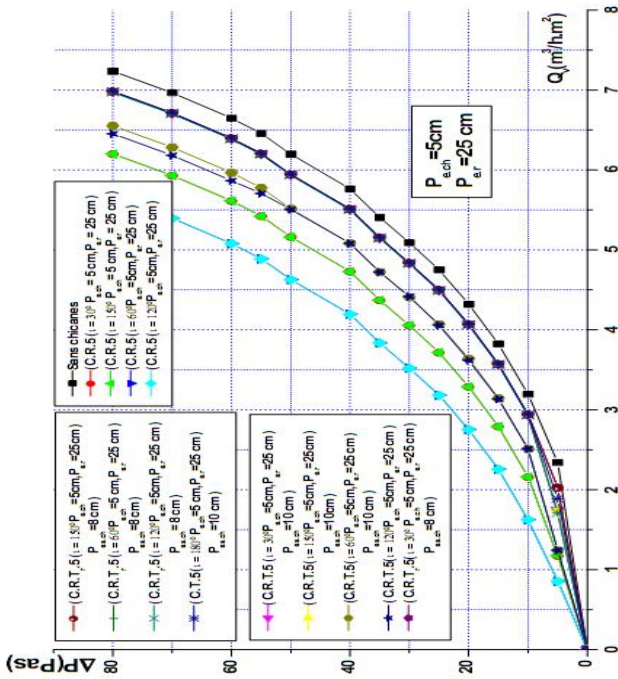


Figure 5: Pressure drop versus flow volume for the effects of 30 °, 60 °, 120 and 150 ° of the inclined part of the baffles arranged in rows or staggered in relation to a smooth duct.

3.1 Case of ribs rectangular – triangular arranged in rows in turbulent

By identifying the geometric parameters of ribs and with reference to the experimental result, the relationship (5) in its expanded form gives us table (1), which for each value of ΔP measured provides a system of equations to solve.

Table 1: Head losses recorded according to geometric parameters considered in the presence of the provision row of baffles (turbulent)

ΔP (Pa)	70	80	70	60	80	80
V (m/s)	0.2080	0.2107	0.2053	0.1883	0.1880	0.2138
ε (m)	0.0299	0.0299	0.0175	0.0299	0.0175	0.0175
L_{ch} (m)	0.05	0.05	0.1	0.1	0.05	0.05
P_{e-ch} (m)	0.05	0.1	0.05	0.05	0.05	0.05
P_{e-r} (m)	0.25	0.25	0.18	0.18	0.05	0.25
P_{e-sch} (m)	0.1	0.15	0.15	0.15	0.1	0.1
D_H (m)	0.0288	0.0329	0.0301	0.0269	0.0317	0.0317

Using the data in Table (1), and referring to the relationship (5) we obtain the following system of equations:

$$\begin{bmatrix} -8.7747 & -0.5963 & 0.4535 & 2.0629 & 0.4535 & 1.1466 \\ -8.6931 & -0.2267 & 0.5502 & 2.1596 & 0.5502 & 1.2433 \\ -8.8422 & -0.3613 & 0.4535 & 1.7344 & 0.4535 & 1.1466 \\ -8.4228 & 0.5419 & 0.5078 & 1.7887 & 1.2010 & 1.6064 \\ -8.5882 & -0.1597 & 0.6172 & 1.8981 & 1.3104 & 1.7158 \\ -8.6904 & -0.5963 & 0.4535 & 0.4535 & 0.4535 & 1.1466 \\ \dots & \dots & \dots & \dots & \dots & \dots \\ \dots & \dots & \dots & \dots & \dots & \dots \end{bmatrix} \begin{bmatrix} x \\ y \\ z \\ t \\ w \\ n \end{bmatrix} = \begin{bmatrix} -3.1129 \\ -3.2420 \\ -2.0164 \\ -3.0442 \\ -3.1720 \\ -3.2768 \\ \dots \\ \dots \end{bmatrix}$$

This is a matrix of 120 lines (n = 120) and of 06 columns (j = 6), which can be written as:

$$\begin{matrix} \mathbf{A}_{i,j} X = B \\ i = 1, \dots, n & / n = 120 \\ j = 1, \dots, 6 \end{matrix}$$

The matrix $\mathbf{A}_{i,j}$ is not square, with a resolution made by the method of least square, therefore:

$$\begin{matrix} \mathbf{A}_{i,j}^T \mathbf{A}_{i,j} X = \mathbf{A}_{i,j}^T B \\ i = 1, \dots, n & / n = 120 \\ j = 1, \dots, 6 \end{matrix}$$

With $\mathbf{A}_{i,j}^T$ is the matrix transpose of $\mathbf{A}_{i,j}$.

This gives a system of equations of the form:

$$\begin{matrix} \mathbf{C}_{i,j} X = D \\ i = 1, \dots, 6 \\ j = 1, \dots, 6 \end{matrix}$$

The solution of this system is determined by the method of Gauss elimination.

After substitution solutions in equation (3)' we get the following correlation which can be applied to the provision of ribs row in the turbulent regime:

$$\Delta P = \frac{LV^2 \rho}{2D_H} \left[\begin{matrix} (\text{Re})^{-1.2060} \left(\frac{\varepsilon}{D_H} \right)^{-0.0043} \left(\frac{P_{e-ch}}{D_H} \right)^{-7.1129} \\ \times \left(\frac{P_{e-r}}{D_H} \right)^{-0.0949} \left(\frac{L_{ch}}{D_H} \right)^{-7.2345} \left(\frac{P_{e-sch}}{D_H} \right)^{12.3519} \end{matrix} \right] \quad (6)$$

$$\lambda = \left[\begin{matrix} (\text{Re})^{-1.2060} \left(\frac{\varepsilon}{D_H} \right)^{-0.0043} \left(\frac{P_{e-ch}}{D_H} \right)^{-7.1129} \\ \times \left(\frac{P_{e-r}}{D_H} \right)^{-0.0949} \left(\frac{L_{ch}}{D_H} \right)^{-7.2345} \left(\frac{P_{e-sch}}{D_H} \right)^{12.3519} \end{matrix} \right] \quad (7)$$

For laminar flow $\text{Re} \leq 2100$, in the presence of the same configuration of the ribs, we obtain the following expression:

$$\Delta P = \frac{L \rho V^2}{2D_H} \left[\begin{matrix} (\text{Re})^{-1.1972} \left(\frac{\varepsilon}{D_H} \right)^{0.7207} \times \\ \left(\frac{P_{e-ch}}{D_H} \right)^{-6.7089} \left(\frac{P_{e-r}}{D_H} \right)^{-0.3428} \\ \times \left(\frac{L_{ch}}{D_H} \right)^{-6.3749} \left(\frac{P_{e-sch}}{D_H} \right)^{11.2249} \end{matrix} \right] \quad (8)$$

With a ratio λ of losses is the term in brackets.

3.2 Case of rectangulo-triangular ribs arranged in staggered rows

Similarly we proceed with the staggered arrangement which gives us:

Turbulent regime

$$\Delta P = \frac{L \rho V^2}{2D_H} \left[\begin{matrix} (\text{Re})^{-1.3912} \left(\frac{\varepsilon}{D_H} \right)^{0.0244} \left(\frac{P_{e-ch}}{D_H} \right)^{-8.7666} \times \\ \left(\frac{P_{e-r}}{D_H} \right)^{0.0805} \left(\frac{L_{ch}}{D_H} \right)^{-8.8184} \left(\frac{P_{e-sch}}{D_H} \right)^{15.0836} \end{matrix} \right] \quad (9)$$

Laminar regime

$$\Delta P = \frac{1}{2} \frac{L}{D_H} \rho \left[\begin{matrix} (\text{Re})^{-1.6915} \left(\frac{\varepsilon}{D_H} \right)^{0.6319} \left(\frac{P_{e-ch}}{D_H} \right)^{-9.6765} \\ \left(\frac{P_{e-r}}{D_H} \right)^{-0.1881} \left(\frac{L_{ch}}{D_H} \right)^{-9.2643} \left(\frac{P_{e-sch}}{D_H} \right)^{16.4783} \end{matrix} \right] V^2 \quad (10)$$

For the other configurations, the values of exponents as expressed by equation (3) corresponding to each baffle configuration, are from table. (1) Summary.

The curve analysis of the evolution ratio losses λ according to Reynolds fig (6) the configurations of the studied ribs shows the good agreement with the models of Blasus [8] for smooth duct and of S.K.Verma et al [9], Chaube et al and Bhagoria et al of which demonstrates the affinity of empirical approaches developed with those cited in the literature.

Table 2: Exhibitors of the correlation corresponding to baffles rectangular.

$$[(R)_f]^{-x} \left(\frac{\varepsilon}{D_H}\right)^y \left(\frac{P_{e,cb}}{D_H}\right)^z \left(\frac{P_{e,r}}{D_H}\right)^t \left(\frac{L_{cb}}{D_H}\right)^w$$

Configuration of ribs	Laminare regime	Turbulent regime	
	Row Layout		
	x	0.2928	0.2985
	y	0.7984	-0.7452
	z	2.2582	-0.0299
	t	-1.3196	-0.3975
	w	-0.2640	-0.3246
Rectangular rib	Staggered arrangement		
	x	1.2697	0.4150
	y	-3.8416	-1.2540
	z	3.2451	0.2820
	t	-0.3260	-0.1972
	w	3.3346	-0.0415

Table 3: Exhibitors of the correlation corresponding to baffles triangular.

$$[(R)_f]^{-x} \left(\frac{\varepsilon}{D_H}\right)^y \left(\frac{P_{e,cb}}{D_H}\right)^z \left(\frac{P_{e,r}}{D_H}\right)^t \left(\frac{L_{cb}}{D_H}\right)^m \left(\frac{P_{e,cb}}{D_H}\right)^n$$

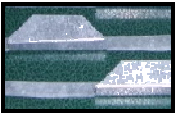
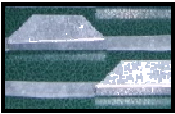
Configuration of ribs	Laminare regime	Turbulent regime	
	Row Layout		
	x	0.9494	0.7902
	y	-0.4095	-0.4748
	z	-4.7993	-4.0636
	t	-0.3016	-0.0787
	w	-2.7847	-2.5227
	n	8.4554	7.3355
Rectangulo –Trapezoidal rib	Staggered arrangement		
	x	0.0048	0.2819
	y	0.6724	-0.3563
	z	0.4630	0.5277
	t	-0.7872	-0.1789
	w	-1.0012	0.0295
	n	-0.2933	-0.6415

Table 4: Exhibitors of the correlation corresponding to baffles rectangulo-trapezoidal

$$[(R)_f]^{-x} \left(\frac{\varepsilon}{D_H}\right)^y \left(\frac{P_{e,cb}}{D_H}\right)^z \left(\frac{P_{e,r}}{D_H}\right)^t \left(\frac{L_{cb}}{D_H}\right)^m \left(\frac{P_{e,cb}}{D_H}\right)^n$$

Configuration of ribs	Laminare regime	Turbulent regime
	Row Layout	
x	0.9494	0.7902
y	-0.4095	-0.4748
z	-4.7993	-4.0636
t	-0.3016	-0.0787
w	-2.7847	-2.5227
n	8.4554	7.3355

Rectangulo – Trapezoidal rib	Staggered arrangement		
	x	0.0048	0.2819
	y	0.6724	-0.3563
	z	0.4630	0.5277
	t	-0.7872	-0.1789
	w	-1.0012	0.0295
	n	-0.2933	-0.6415

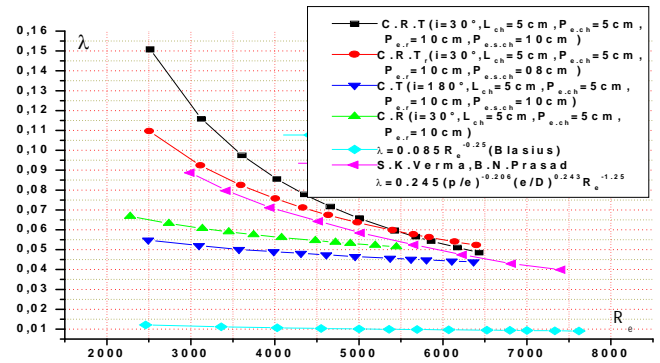


Figure 6: Coefficient of pressure losses λ according to Reynolds empirical models, in comparison with the model of (Blasius) and (S.K.Verma et al) baffles in rows.

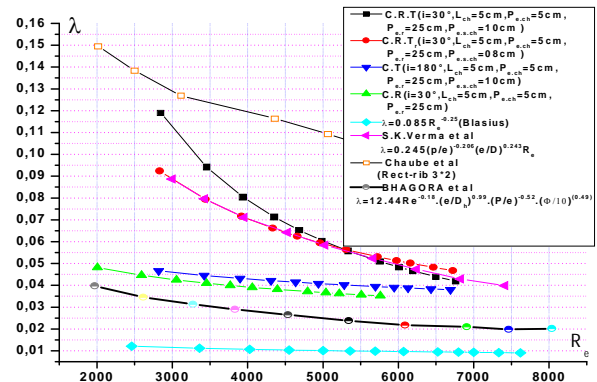


Figure 7: Coefficient of pressure losses λ according to Reynolds empirical models, in comparison with the model of (Blasius), (S.K.Verma), (Chaube et al) and (Bhagoria et al), baffles in rows.

4 CONCLUSION

From this experimental study, we were able to identify empirical relationships between load losses and geometric properties of four configurations of baffles. These correlations are used to measure the pressure drop in a rectangular duct fitted with studied ribs. The results obtained show that the pressure drop between the upstream and downstream of the pipe is even greater in the presence of the staggered arrangements, especially with high incidences of the inclined part.

The optimization of convective exchanges by adding artificial roughness is in spite of mechanical power for pumping the coolant; however it is interesting to consider other forms of optimal configurations, which achieve the

best compromise between energetic performance and energy loss of mechanical power.

Bibliography

- [1] J.L .Bhagoria, J.S. Saini, S.C. Solanki , Heat transfer coefficient and friction factor correlations for rectangular solar air heater duct having transverse wedge shaped rib roughness on the absorber plate .Renew Energy 2002;25 (3) :341-69.
- [2] R.Karwa ,S.C.Solanki , J.S.Saini, Heat transfer coefficient and friction factor correlations for the transient flow regime in rib –roughened rectangular ducts ,Int .J.Heat Mass Transfer 42 (1999) 1597 -1615.
- [3] A.Chaube,P.K.Sahoo,S.C.Solanki , Analysis of heat transfer augmentation and flow characteristics due to rib roughness over absorber plate of a solar air heater .Renew Energy 2006 ;(3) m317 -31 .
- [4] Apura Layek , J.S.Saini ,S.C.Solanki , Heat transfer and friction characteristics for artificially roughened ducts with compound turbulators .I.J.of heat and Mass Transfer 50 (2007) 4845 -4854 .
- [5] D.Cavallero , G.Tanda , An experimental investigation of forced convection heat transfer in channels with rib turbulators by means of liquid crystal thermography . Experimental Thermal and Fluid Science 26 (2002) 115 - 121.
- [6] G.Tanda, Heat transfer in rectangular channels with transverse and V-shaped broken ribs. I.J.of heat and Mass Transfer 47 (2004) 229 -243.
- [7] A.R.Jauker, J.S.Saini, B.K.Gandhi, Heat transfer and friction characteristics of rectangular solar air heater duct using – grooved artificial roughness .Solar Energy; 80(8) m895-907.
- [8] B.N.Prasad , J.S.Saini, effect of artificial roughness on heat transfer and friction factor in a solar air heater , Solar Energy 41 (1988) 555 -560 .
- [9] S.K.Verrma,*, B.N. Prasad. Investigation for the optimal thermohydraulic performance of artificially roughened solar air heaters. Renewable Energy Vol.20 pp.19-36. (2000).
- [10] M.Carlier, *Hydraulique Générale et Appliquée*, Edition Eyrolles Paris 1986.
- [11] B.B.Prasad et J.S.Saini, Optimal thermohydraulic performance of artificially roughened solar air heating, Solar Energy Vol.47, N°2, pp.91-96 (1991).
- [12] B.B.Prasad et J.S.Saini, Effect of artificial roughness on heat transfer and friction factor in solar air-heaters, Solar Energy Vol.41, N°6. pp.505-560 (1980).
- [13] A.Moummi, Etude globale et locale du rôle de la géométrie dans l'optimisation des capteurs solaires plans à air, Thèse de doctorat, Université de Valenciennes, France 1994.
- [14] N.Chouchane, Modélisation des pertes de charge dans un conduit rectangulaire garni de rugosités artificielles avec une partie supérieure inclinée, Mémoire de Magister, Université de Biskra, Algérie 2003.
- [15] Webb RL. Air-side heat transfer correlations for flat and wavy plate fin-and-tube geometries. ASHRAE Transaction Vol.96 (2) pp.445-449. (1990)
- [16] Chi-Chuan Wang et Young-Ming Hwang. Corrélations empiriques relatives au transfert de chaleur et aux pertes par frottement pour des échangeurs à tubes ailettes, avec ailettes ondulées. International Journal of Refrigeration Vol.25 pp.673-680. (2002)
- [17] Mohamed Mahfoud, Salah Benhadid, Michel Lebouché. Frottements et pertes de charge des fluides viscoélastiques dans des conduites rectangulaires. Heat and Mass transfer 17 February 2006.
- [18] C.C.Wanga,J-Y, Jang, N.F-Chioub. A heat transfer and friction correlation for wavy and tube heat exchangers. International Journal of Heat and Mass Transfer Vol.42 pp.1919-1924.(1999)
- [19] Dong Junqi , Chen Jiangping, Chen Zhijiu, Zhou Yimin, Zhang Wenfeng. Heat transfer and pressure drop correlations for the wavy fin and flat tube heat exchangers. Applied Thermal Engineering Vol.27 2066-2073. (2007).
- [20] Apura Layek , J.S.Saini ,S.C.Solanki , Effect of chamfering on heat transfer and friction characteristics of solar air heater having absorber plate roughened with compound turbulators .Renewable Energy 34 (2009) 1292 -1298